



**HAL**  
open science

## Europium Nitride: A Novel Diluted Magnetic Semiconductor

Do Le Binh, B. J. Ruck, F. Natali, H. Warring, H. J. Trodahl, E. M. Anton, Claire Meyer, Laurent Ranno, F. Wilhem, Andrei Rogalev

► **To cite this version:**

Do Le Binh, B. J. Ruck, F. Natali, H. Warring, H. J. Trodahl, et al.. Europium Nitride: A Novel Diluted Magnetic Semiconductor. *Physical Review Letters*, 2013, 111, pp.167206. 10.1103/PhysRevLett.111.167206 . hal-00962328

**HAL Id: hal-00962328**

**<https://hal.science/hal-00962328>**

Submitted on 21 Mar 2014

**HAL** is a multi-disciplinary open access archive for the deposit and dissemination of scientific research documents, whether they are published or not. The documents may come from teaching and research institutions in France or abroad, or from public or private research centers.

L'archive ouverte pluridisciplinaire **HAL**, est destinée au dépôt et à la diffusion de documents scientifiques de niveau recherche, publiés ou non, émanant des établissements d'enseignement et de recherche français ou étrangers, des laboratoires publics ou privés.

## Europium Nitride: A Novel Diluted Magnetic Semiconductor

Do Le Binh,<sup>1</sup> B. J. Ruck,<sup>1,\*</sup> F. Natali,<sup>1</sup> H. Warring,<sup>1</sup> H. J. Trodahl,<sup>1</sup> E.-M. Anton,<sup>1</sup> C. Meyer,<sup>2</sup> L. Ranno,<sup>2</sup>  
F. Wilhelm,<sup>3</sup> and A. Rogalev<sup>3</sup>

<sup>1</sup>*The MacDiarmid Institute for Advanced Materials and Nanotechnology, School of Chemical and Physical Sciences, Victoria University of Wellington, P.O. Box 600, Wellington 6140, New Zealand*

<sup>2</sup>*Institut Néel, Centre National de la Recherche Scientifique and Université Joseph Fourier, Boîte Postale 166, F-38042 Grenoble Cedex, France*

<sup>3</sup>*European Synchrotron Radiation Facility, Boîte Postale 220, F-38043 Grenoble Cedex, France*

(Received 30 June 2013; published 18 October 2013)

Europium nitride is semiconducting and contains nonmagnetic  $\text{Eu}^{3+}$ , but substoichiometric  $\text{EuN}$  has  $\text{Eu}$  in a mix of  $2+$  and  $3+$  charge states. We show that at  $\text{Eu}^{2+}$  concentrations near 15%–20%  $\text{EuN}$  is ferromagnetic with a Curie temperature as high as 120 K. The  $\text{Eu}^{3+}$  polarization follows that of the  $\text{Eu}^{2+}$ , confirming that the ferromagnetism is intrinsic to the  $\text{EuN}$  which is, thus, a novel diluted magnetic semiconductor. Transport measurements shed light on the likely exchange mechanisms.

DOI: [10.1103/PhysRevLett.111.167206](https://doi.org/10.1103/PhysRevLett.111.167206)

PACS numbers: 75.25.-j, 75.47.-m, 75.50.Pp

Diluted magnetic semiconductors, in which magnetic impurities are doped into a semiconducting host, offer important opportunities for use in spintronics technology as materials for spin injection or manipulation [1–3]. Understanding the exchange interactions in these systems is challenging, with a range of theoretical models proposed to describe the various systems [3–6]. The understanding is further complicated by the possible existence of magnetic impurity phases distinct from the semiconducting host, as these can often be of small enough dimensions to escape conventional detection methods [7–10]. Nevertheless, numerous examples of diluted magnetic semiconductor systems have been reported, with ferromagnetic transition temperatures ranging from a few kelvin to far above room temperature [11–13]. In the most well studied system, Mn-doped III-V semiconductors, the exchange mechanism is now reasonably well understood based on the modified Zener model of coupling mediated by carriers [3].

By contrast, it is relatively rare to find intrinsically ferromagnetic semiconductors, where the ordered magnetic moments are provided directly by the host cations [14–16]. The most notable example is  $\text{EuO}$  [15], where the physics of the magnetic state in electron-doped samples remains controversial [17,18]. The rare-earth nitride series, which is largely ionic with  $3+$  valence for the rare-earth and  $3-$  for nitrogen, also contain such intrinsic ferromagnetic semiconductors, including  $\text{GdN}$ ,  $\text{DyN}$ , and  $\text{SmN}$  [19–24]. Europium nitride has also been demonstrated to be semiconducting [25], but  $\text{EuN}$  stands out amongst the rare-earth nitrides because the ground state of the  $\text{Eu}^{3+}$  ion has configuration  $4f^6$  giving it a total angular momentum  $J = 0$ , and thus, it is nonmagnetic [26]. Accordingly, there are no ferromagnetic compounds based on  $\text{Eu}^{3+}$ . However, trivalent  $\text{Eu}$  does possess a nonzero spin angular momentum quantum number  $S = 3$  which has led to the suggestion that it might support “hidden ferromagnetism” [26].

Furthermore, the first excited state  $J = 1$  lies close in energy to the ground state, so  $\text{Eu}^{3+}$  has a relatively strong van Vleck susceptibility [27]. Thus, the magnetic properties of stoichiometric or doped  $\text{EuN}$  are of substantial interest.

We have previously demonstrated that epitaxial  $\text{EuN}$  films display a dominant paramagnetic signal that is at odds with that expected for a collection of  $\text{Eu}^{3+}$  ions [28]. The origin of this signal was shown to be a concentration of a few percent of  $\text{Eu}^{2+}$ , most likely related to doping by nitrogen vacancies in the material [25]. Furthermore, x-ray magnetic circular dichroism (XMCD) at the  $\text{Eu}$   $L$  edges showed that there is a partial polarization of the  $\text{Eu}^{3+}$  that follows the  $\text{Eu}^{2+}$  polarization [28].

It is of fundamental interest to investigate the evolution of the magnetism in  $\text{EuN}$  as the quantity of  $\text{Eu}^{2+}$  increases, thereby increasing the possibility of interaction between the localized magnetic moments. Here, we present such a study based on  $\text{EuN}$  films with  $\text{Eu}^{2+}$  concentrations as high as 15%–20%, and we show that such films are ferromagnetic at temperatures well above 100 K. XMCD results show that the  $\text{Eu}^{2+}$  ions polarize the neighboring  $\text{Eu}^{3+}$ , showing that the ferromagnetism is not an artefact of an impurity phase and suggesting that  $\text{Eu}^{3+}$  plays a role in the exchange mechanism.

The 100–200 nm thick  $\text{EuN}$  films were grown onto substrates of either sapphire or  $\text{GaN}$  templates on sapphire by thermal evaporation of  $\text{Eu}$  in the presence of a flux of ionized nitrogen. In contrast to other rare-earth nitrides, the use of an excited nitrogen source is essential for obtaining near-stoichiometric  $\text{EuN}$  films. The nitrogen partial pressure in the growth chamber was  $3\text{--}5 \times 10^{-4}$  mbar and the ions were accelerated through 125 V at a beam current of 0.37 mA. The films were grown at either room temperature or 680 °C, and were capped to prevent oxidation after growth using layers of either  $\text{GaN}$  or  $\text{AlN}$ . The films

were characterized by reflection high-energy electron diffraction and x-ray diffraction, which showed that the 680 °C grown films are epitaxial with [111] orientation, while the room temperature grown films are polycrystalline with [111] texturing. There is no evidence in the x-ray diffraction for any impurity phase, and all films show the expected lattice constant of 4.99 Å [25,29,30]. As we will show below, the key difference between the 680 °C and the room temperature grown films is that the latter are more heavily doped and contain a substantially larger  $\text{Eu}^{2+}$  concentration. We show representative data from films grown at the two temperatures, but the repeatability of the magnetization and transport results has been checked on additional samples grown under similar conditions.

The magnetization of the films was measured using a Quantum Design MPMS SQUID magnetometer. Further investigation of the magnetic state of the films was made by XMCD carried out at beam line ID12 of the European Synchrotron Radiation Facility in Grenoble, France. Measurements were made at grazing incidence in the total fluorescence yield detection mode, with the magnetic field applied in the film plane. Electrical transport measurements were conducted in a Quantum Design Physical Properties Measurement System using a four terminal geometry with contacts made using pressed indium.

In Figure 1 we show our main result, namely, that the room temperature grown films are ferromagnetic with a Curie temperature near 120 K as evidenced by the sharp rise in the temperature dependent magnetization. A clear hysteresis is observed at low temperatures (Fig. 1 inset) along with saturation of the magnetization at around  $1.4 \mu_B$  per Eu ion. The field-cooled (FC) and zero-field-cooled (ZFC) curves separate below about 50 K, marking the point below which the coercive field exceeds the 500 Oe measurement field. Assuming the magnetic

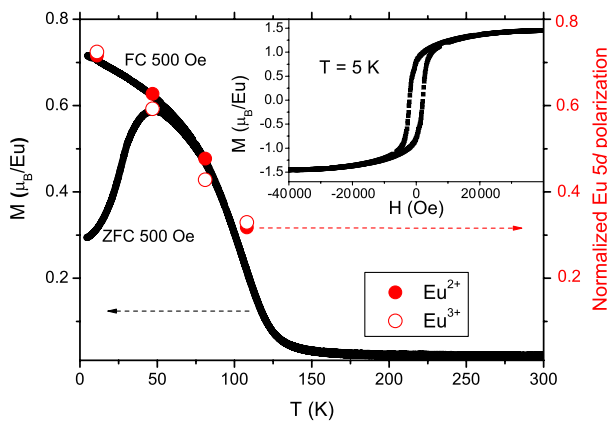


FIG. 1 (color online). Field cooled and zero field cooled temperature dependent magnetization of a room temperature grown EuN film (solid lines) measured in a field of 500 Oe. Also shown are the  $\text{Eu}^{2+}$  and  $\text{Eu}^{3+}$  XMCD amplitudes (solid and open circles), which both follow the measured magnetization. Inset: Hysteresis loop measured at 5 K.

response is associated with the  $\text{Eu}^{2+}$  component of the film, we estimate a rather large divalent fraction corresponding to about 20% of the cations. A series of similar room temperature grown films all showed ferromagnetism, with Curie temperatures ranging from 100 to 120 K (estimated by extrapolating the steepest part of the magnetization curve back to zero). By contrast the 680 °C grown films display only a paramagnetic response whose magnitude is consistent with  $\text{Eu}^{2+}$  concentrations of around 2%–5%.

To understand the origin of the ferromagnetism, we have carried out XMCD on a ferromagnetic EuN film grown at room temperature. The  $L_{2,3}$ -edge XMCD involves the transition  $2p^65d^0 \rightarrow 2p^55d^1$  so it interrogates the polarization of the  $5d$  empty-state conduction band orbitals. The x-ray absorption spectrum at the  $L_2$  edge shown in Figure 2(a) shows a clear shoulder at 7615 eV superimposed on the usual  $\text{Eu}^{3+}$  white line absorption centered at 7624 eV. Atomic multiplet calculations clearly identify the shoulder as originating from absorption by  $\text{Eu}^{2+}$  ions [25,31]. This feature is substantially stronger than the corresponding shoulder seen in a paramagnetic epitaxial EuN film [28], confirming the much larger  $\text{Eu}^{2+}$  concentration in the room temperature grown films. The curve fitting of the 2+ and 3+ peaks shown in the figure implies a  $\text{Eu}^{2+}$  concentration of around 15%, consistent within uncertainty with the value extracted above from the saturation magnetization.

The corresponding XMCD spectra taken at various temperatures in a field of 3 T are also plotted in Fig. 2(a). The strongest feature near 7615 eV is clearly associated with  $\text{Eu}^{2+}$ . The strength of this XMCD feature at the lowest temperature is roughly three times stronger than in the paramagnetic epitaxial films [28], and its temperature dependence follows closely the measured magnetization as shown by the solid symbols in Fig. 1 (the disagreement between the SQUID and XMCD amplitudes at 105 K is a result of the much higher measurement field used for XMCD). These observations confirm the origin of the ferromagnetism to be the Eu in the film.

The remainder of the XMCD features are associated mostly with  $\text{Eu}^{3+}$ , and, interestingly, these also show a strong signature of the ferromagnetism. Similar to the  $\text{Eu}^{2+}$  XMCD, the amplitude of the 3+ signal is much larger than that seen in paramagnetic films at similar applied fields. Furthermore, rather than following a van Vleck temperature dependence, the  $\text{Eu}^{3+}$  signal closely follows the  $\text{Eu}^{2+}$  signal (open symbols in Fig. 1), implying that there is a strong exchange coupling between the  $\text{Eu}^{2+}$  and  $\text{Eu}^{3+}$  ions [32]. This is further demonstrated in Fig. 2(b) which shows the  $\text{Eu}^{3+}$  polarization plotted against the  $\text{Eu}^{2+}$  polarization determined from the XMCD using the method described in Ref. [28]. The red triangles represent data from the paramagnetic sample of Ref. [28]. The black circles, representing the ferromagnetic

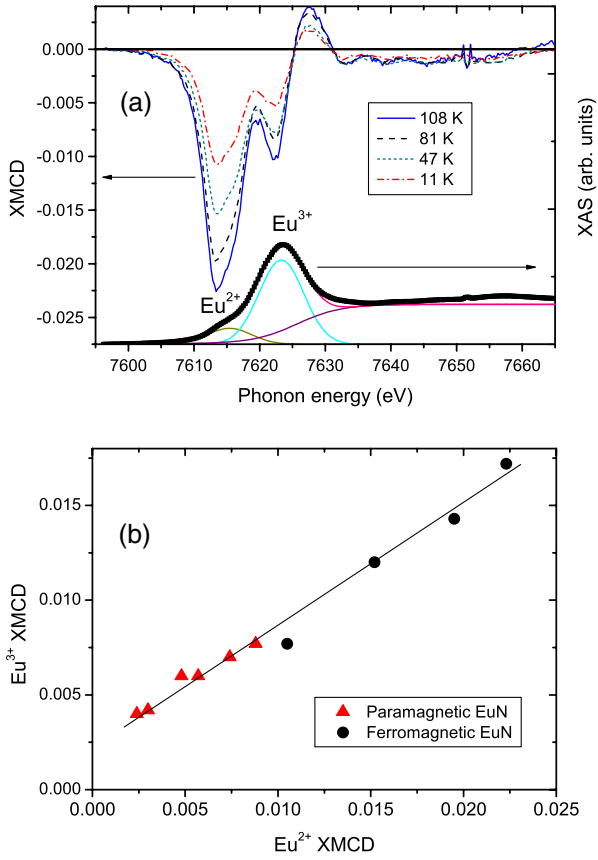


FIG. 2 (color online). (a) Eu  $L_2$ -edge x-ray absorption and XMCD at various temperatures from ferromagnetic EuN. The fit to the absorption spectrum (thin solid lines) implies that about 15% of the Eu ions are in the 2+ charge state. Strong XMCD with similar temperature dependence is observed for both the  $\text{Eu}^{2+}$  and  $\text{Eu}^{3+}$  features. (b)  $\text{Eu}^{3+}$  versus  $\text{Eu}^{2+}$  polarization of the  $5d$  electrons extracted from the XMCD spectra. The black circles are from the ferromagnetic film in (a), the red triangles from the paramagnetic film reported in Ref. [28]. The solid line is a guide to the eye.

sample, show much larger polarization for both species, but they follow the same trend as the paramagnetic sample implying that the coupling between the  $\text{Eu}^{2+}$  and  $\text{Eu}^{3+}$  ions is of the same nature in each case, with the key difference simply being the concentration. We stress that the strong coupling between the  $\text{Eu}^{2+}$  and  $\text{Eu}^{3+}$  is compelling evidence that the ferromagnetic phase is not simply an impurity, such as electron-doped EuO [15,18], but rather represents the response of the EuN matrix containing a large concentration of  $\text{Eu}^{2+}$  ions.

We have further investigated the source of the doping and the nature of the exchange mechanism that couples the  $\text{Eu}^{2+}$  by measuring the transport properties of the films. Figure 3(a) shows the temperature dependent resistivity of a room temperature grown ferromagnetic film and a paramagnetic film grown at  $680^\circ\text{C}$ . The paramagnetic film shows a metallic temperature dependence at high temperature, developing a negative temperature coefficient of

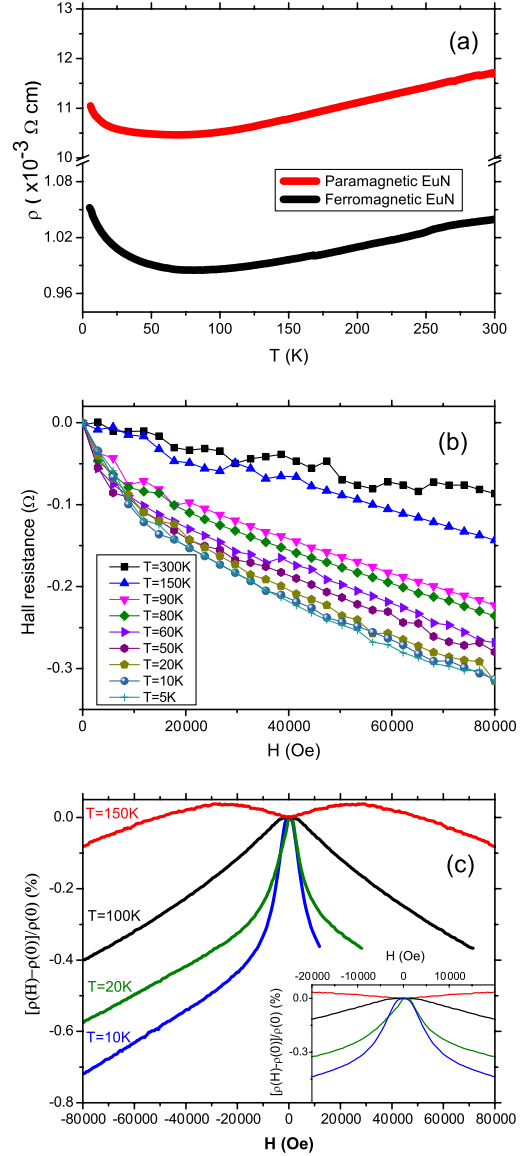


FIG. 3 (color online). (a) Temperature dependent resistivity of ferromagnetic (black) and paramagnetic (red) EuN. (b) Hall resistance of ferromagnetic EuN, showing an anomalous Hall effect below the  $T_C$  of 120 K. (c) Magnetoresistance of ferromagnetic EuN showing cusplike behavior at low fields for temperatures below  $T_C$ . Inset: Low-field magnetoresistance.

resistance below about 60 K. The magnitude of the resistivity is rather high ( $\approx 11 \text{ m}\Omega \text{ cm}$ ), consistent with the conclusion that these EuN films are semiconductors doped to degeneracy by a high concentration of nitrogen vacancies. This is further supported by Hall effect measurements that give a carrier concentration at room temperature of  $-8 \times 10^{20} \text{ cm}^{-3}$  (i.e., the carriers are electrons). The origin of the upturn in the resistivity below 60 K is uncertain. Magnetic scattering from the  $\text{Eu}^{2+}$  in the film could lead to a Kondo effect [33,34], and indeed, the resistivity does follow the expected logarithmic temperature dependence.

The room temperature grown ferromagnetic film shows a qualitatively similar temperature dependent resistivity, although the magnitude is substantially smaller and the carrier concentration is larger ( $4 \times 10^{21} \text{ cm}^{-3}$ ). The ratio of carrier concentration between the two films is similar to the ratio of  $\text{Eu}^{2+}$  content, indicating a link between the two quantities. The low temperature resistivity upturn occurs at higher temperature in the ferromagnetic sample than the paramagnetic sample, and it constitutes a larger fractional change in resistivity in the film with more  $\text{Eu}^{2+}$ . However, the ferromagnetic film has a larger mobility ( $1.5 \text{ cm}^2 \text{ V}^{-1} \text{ s}^{-1}$ ) than the paramagnetic film ( $0.7 \text{ cm}^2 \text{ V}^{-1} \text{ s}^{-1}$ ), supporting the conclusion that the upturn is related to magnetic scattering rather than weak localization [35].

There is no sharp anomaly at the Curie temperature in the ferromagnetic sample, as is often observed in ferromagnets where it can be caused either by scattering from magnetic fluctuations [34,36,37] or by a change in carrier concentration as the sample enters the ferromagnetic state [15,19,20]. On the other hand evidence for the magnetic ordering is clearly seen in the form of an anomalous Hall effect that sets in below  $T_C$  [Fig. 3(b)], the strength of which is enhanced by the relatively large resistivity in these films. Evidence for coupling between the magnetic order and the electrical transport is also present in the magnetoresistance presented in Fig. 3(c). It shows a negative parabolic behavior above  $T_C$ , characteristic of scattering from uncorrelated magnetic impurities [38], with an additional positive contribution evident at low field [10]. These features disappear below  $T_C$  to be replaced by a sharp negative cusp at low fields followed by a near-linear high-field behavior, similar to the behavior observed in other ferromagnets [39]. By contrast, the magnetoresistance of the paramagnetic sample is parabolic down to low temperature with a small cusp observable only below 10 K. Similarly, the paramagnetic films show evidence for an anomalous Hall effect only below 10 K where the  $\text{Eu}^{2+}$  becomes strongly polarized in the large measurement fields.

Based on the evidence presented above and previous calculations and measurements of the electronic structure of stoichiometric  $\text{EuN}$ , we propose a simple model for the formation of  $\text{Eu}^{2+}$  in  $\text{EuN}$ . The underlying band structure is semiconducting, but with the  $\text{Eu}^{2+} 4f^7$  ( $^8S$ ) level lying very close to the bottom of the conduction band [25]. The presence of large quantities of nitrogen vacancies shifts the Fermi level into the conduction band, and at carrier concentrations above  $\sim 10^{20} \text{ cm}^{-3}$  it approaches the  $^8S$  level that, thus, becomes populated. This is similar to a proposed model of the electronic structure of substoichiometric  $\text{YbN}$  [40], although there the  $\text{Yb}^{2+}$  is nonmagnetic and there is no magnetic ordering.

Given the above model, it is interesting to seek evidence for an enhancement of the effective mass in the heavily doped samples where the Fermi level approaches the  $\text{Eu}^{8S}$

level. To investigate this possibility we write the resistivity as the sum of a phonon contribution ( $\rho_{\text{ph}}$ ) and a contribution from disorder scattering involving both lattice defects and magnetic inhomogeneity ( $\rho_{\text{dis}}$ )

$$\rho(T) = \rho_{\text{dis}} + \rho_{\text{ph}} = \frac{m^*}{ne^2\tau_{\text{dis}}} + \frac{m^*}{ne^2\tau_{\text{ph}}}, \quad (1)$$

where  $m^*$  is the carrier effective mass,  $n$  is the carrier concentration,  $e$  is the electron's charge,  $\tau_{\text{ph}}$  is the phonon scattering time, and  $\tau_{\text{dis}}$  is the combined magnetic and quenched disorder scattering time. At high temperature,  $\tau_{\text{dis}}$  is temperature independent and the phonon scattering rate  $\tau_{\text{ph}}^{-1} = cT$  with  $c$  a constant, so we can express the effective mass as

$$m^* = \frac{1}{ne^2c} \frac{d\rho}{dT}. \quad (2)$$

Assuming the phonon scattering rate, and hence the constant  $c$ , is the same in all samples, and using the measured resistivity slopes and carrier concentrations, we can seek variations in  $m^*$  between samples. Doing so we find that the paramagnetic film in Fig. 3(a) has a larger  $m^*$  than the ferromagnetic film by a factor of nearly 3. This is the same within the uncertainty among all of the films, and we see no evidence for a systematic variation in  $m^*$  with  $\text{Eu}^{2+}$  concentration. Once again, this is consistent with conclusions obtained from  $\text{YbN}$  [40].

Next, we consider the possible exchange interactions present in the films. The carrier concentration in the ferromagnetic samples is larger than in the paramagnetic films, suggesting that carrier mediated mechanisms may play an important role. Indeed, the conduction band states are formed primarily from  $\text{Eu} 5d$  orbitals, and the XMCD results show a very clear polarization of these states. This is similar to the polarization of  $\text{Eu}^{3+}$  seen in the mixed valence compounds  $\text{EuNi}_2\text{P}_2$  and  $\text{EuNi}_2(\text{Si}_{0.18}\text{Ge}_{0.82})_2$ , although there the polarization was induced by a very large applied field [32]. At the large  $\text{Eu}^{2+}$  concentrations where ferromagnetism occurs, there will be many nearest-neighbor  $\text{Eu}^{2+}$  ions on the cation sublattice, allowing for short-ranged exchange interactions. This will naturally lead to a percolating type of magnetic ordering nucleating at regions of high  $\text{Eu}^{2+}$  density, and this percolating nature might explain the lack of a cusp at  $T_C$  in the temperature dependent resistivity. Finally, we note that the underlying matrix of  $\text{Eu}^{3+}$  ions is also polarizable due to the small energy gap to the  $J = 1$  excited state, which could lead to a Van Vleck type contribution to the exchange interaction as has been reported for Cr-doped  $\text{Bi}_2\text{Sb}_3$  [41]. XMCD measurements at the  $\text{Eu} M$  edge would be of interest to probe the  $4f$  levels directly.

In summary, we have shown that  $\text{EuN}$  with a large fraction of the  $\text{Eu}$  ions in the  $2+$  charge state is ferromagnetic at temperatures as high as 120 K. Thus, it represents a

novel diluted magnetic semiconducting system, with the magnetism contributed largely by the  $\text{Eu}^{2+}$ , but where the host lattice based on  $\text{Eu}^{3+}$  is also polarizable. The concentration of  $\text{Eu}^{2+}$  ions is correlated with the charge carrier concentration, allowing us to propose a simple model for the formation of  $\text{Eu}^{2+}$ . The large concentration of  $\text{Eu}^{2+}$  in the ferromagnetic samples requires that many are nearest neighbors on the cation lattice allowing for short-ranged exchange interactions which may be supported by interactions involving the charge carriers and also even the polarizable  $\text{Eu}^{3+}$  background. The relatively simple physical structure of this system may make it an attractive testing ground for theories of exchange interactions in diluted magnetic systems.

We acknowledge funding from the NZ Foundation for Research, Science, and Technology (Grant No. VICX0808) and the Marsden Fund (Grant No. 08-VUW-030). The MacDiarmid Institute is supported by the New Zealand Centres of Research Excellence Fund. We are grateful to Walter Lambrecht for helpful discussions. E. A. thanks the Alexander von Humboldt foundation for support through a fellowship.

\*ben.ruck@vuw.ac.nz

- [1] D. D. Awschalom and M. E. Flatte, *Nat. Phys.* **3**, 153 (2007).
- [2] I. Žutić, J. Fabian, and S. D. Sarma, *Rev. Mod. Phys.* **76**, 323 (2004).
- [3] T. Dietl, H. Ohno, F. Matsukura, J. Cibert, and D. Ferrand, *Science* **287**, 1019 (2000).
- [4] J. M. D. Coey, M. Venkatesan, and C. B. Fitzgerald, *Nat. Mater.* **4**, 173 (2005).
- [5] A. Zunger, S. Lany, and H. Raebiger, *Physics* **3**, 53 (2010).
- [6] J. M. D. Coey, P. Stamenov, R. D. Gunning, M. Venkatesan, and K. Paul, *New J. Phys.* **12**, 053025 (2010).
- [7] A. Ney, *Materials* **3**, 3565 (2010).
- [8] S. R. Shinde, S. B. Ogale, J. S. Higgins, H. Zheng, A. J. Millis, V. N. Kulkarni, R. Ramesh, R. L. Greene, and T. Venkatesan, *Phys. Rev. Lett.* **92**, 166601 (2004).
- [9] S. Chambers, *Nat. Mater.* **9**, 956 (2010).
- [10] T. Dietl, T. Andrearczyk, A. Lipińska, M. Kiecana, M. Tay, and Y. Wu, *Phys. Rev. B* **76**, 155312 (2007).
- [11] M. Sawicki, T. Devillers, S. Gałęski, C. Simserides, S. Dobkowska, B. Faina, A. Grois, A. Navarro-Quezada, K. N. Trohidou, J. A. Majewski *et al.*, *Phys. Rev. B* **85**, 205204 (2012).
- [12] S. Dhar, O. Brandt, M. Ramsteiner, V. F. Sapega, and K. H. Ploog, *Phys. Rev. Lett.* **94**, 037205 (2005).
- [13] J. Cibert and D. Scalbert, *Spin Physics in Semiconductors*, Springer Series in Solid-State Sciences Vol. 157 (Springer, Berlin, 2008), pp. 389–431.
- [14] E. L. Nagaev and M. Samokhvalov (Translator), *Physics of Magnetic Semiconductors* (Mir, Moscow, 1983).
- [15] A. Mauger and C. Godart, *Phys. Rep.* **141**, 51 (1986).
- [16] S. D. Pappas, P. Pouloupoulos, B. Lewitz, A. Straub, A. Goschew, V. Kapaklis, F. Wilhelm, A. Rogalev, and P. Fumagalli, *Sci. Rep.* **3**, 1333 (2013).
- [17] P. M. S. Monteiro, P. J. Baker, A. Ionescu, C. H. W. Barnes, Z. Salman, A. Suter, T. Prokscha, and S. Langridge, *Phys. Rev. Lett.* **110**, 217208 (2013).
- [18] P. Liu and J. Tang, *Phys. Rev. B* **85**, 224417 (2012).
- [19] F. Leuenberger, A. Parge, W. Felsch, K. Fauth, and M. Hessler, *Phys. Rev. B* **72**, 014427 (2005).
- [20] S. Granville, B. J. Ruck, F. Budde, A. Koo, D. Pringle, F. Kuchler, A. Preston, D. Housden, N. Lund, A. Bittar, G. V. M. Williams, and H. J. Trodahl, *Phys. Rev. B* **73**, 235335 (2006).
- [21] A. R. H. Preston, S. Granville, D. H. Housden, B. Ludbrook, B. J. Ruck, H. J. Trodahl, A. Bittar, G. V. M. Williams, J. E. Downes, A. DeMasi *et al.*, *Phys. Rev. B* **76**, 245120 (2007).
- [22] M. Azeem, B. J. Ruck, B. D. Le, H. Warring, H. J. Trodahl, N. M. Strickland, A. Koo, V. Goian, and S. Kamba, *J. Appl. Phys.* **113**, 203509 (2013).
- [23] C. Meyer, B. J. Ruck, J. Zhong, S. Granville, A. R. H. Preston, G. V. M. Williams, and H. J. Trodahl, *Phys. Rev. B* **78**, 174406 (2008).
- [24] P. Larson, W. R. L. Lambrecht, A. Chantis, and M. van Schilfgaarde, *Phys. Rev. B* **75**, 045114 (2007).
- [25] J. H. Richter, B. Ruck, M. Simpson, F. Natali, N. O. V. Plank, M. Azeem, H. J. Trodahl, A. R. H. Preston, B. Chen, J. McNulty *et al.*, *Phys. Rev. B* **84**, 235120 (2011).
- [26] M. D. Johannes and W. E. Pickett, *Phys. Rev. B* **72**, 195116 (2005).
- [27] J. H. Van Vleck, *The Theory of Electric and Magnetic Susceptibilities* (Oxford University Press, Oxford, 1932).
- [28] B. J. Ruck, H. J. Trodahl, J. H. Richter, J. C. Cezar, F. Wilhelm, A. Rogalev, V. N. Antonov, B. D. Le, and C. Meyer, *Phys. Rev. B* **83**, 174404 (2011).
- [29] W. Klemm and G. Winkelmann, *Z. Anorg. Allg. Chem.* **288**, 87 (1956).
- [30] R. C. Brown and N. J. Clark, *J. Inorg. Nucl. Chem.* **36**, 2507 (1974).
- [31] B. T. Thole, G. van der Laan, J. C. Fuggle, G. A. Sawatzky, R. C. Karnatak, and J.-M. Esteve, *Phys. Rev. B* **32**, 5107 (1985).
- [32] Y. H. Matsuda, Z. W. Ouyang, H. Nojiri, T. Inami, K. Ohwada, M. Suzuki, N. Kawamura, A. Mitsuda, and H. Wada, *Phys. Rev. Lett.* **103**, 046402 (2009).
- [33] J. Kondo, *Prog. Theor. Phys.* **32**, 37 (1964).
- [34] H. T. He, C. L. Yang, W. K. Ge, J. N. Wang, X. Dai, and Y. Q. Wang, *Appl. Phys. Lett.* **87**, 162506 (2005).
- [35] B. L. Altshuler, A. G. Aronov, D. E. Khmel'nitskii, and A. I. Larkin, *Quantum Theory of Solids* (Mir, Moscow, 1982), p. 130.
- [36] P. de Gennes and J. Friedel, *J. Phys. Chem. Solids* **4**, 71 (1958).
- [37] M. E. Fisher and J. S. Langer, *Phys. Rev. Lett.* **20**, 665 (1968).
- [38] M. T. B. Monod and R. A. Weiner, *Phys. Rev.* **170**, 552 (1968).
- [39] M. Csontos, T. Wojtowicz, X. Liu, M. Dobrowolska, B. Jankó, J. K. Furdyna, and G. Mihály, *Phys. Rev. Lett.* **95**, 227203 (2005).
- [40] L. Degiorgi, W. Bacsá, and P. Wachter, *Phys. Rev. B* **42**, 530 (1990).
- [41] R. Yu, W. Zhang, H.-J. Zhang, S.-C. Zhang, X. Dai, and Z. Fang, *Science* **329**, 61 (2010).